Geometry-dependent scattering through quantum billiards: Experiment and theory

T. Blomquist,[1] H. Schanze,[2] I. V. Zozoulenko,[3,1] and H.-J. Stöckmann[2]
[1]*Department of Physics (IFM), Linköping University, S–581 83 Linköping, Sweden*
[2]*Fachbereich Physik, Philipps-Universität Marburg, D-35032 Marburg, Germany*
[3]*Department of Science and Technology (ITN), Linköping University, S–601 74 Norrköping, Sweden*
(Received 24 February 2002; revised manuscript received 17 May 2002; published 28 August 2002)

We present experimental studies of geometry-specific quantum scattering in microwave billiards of a given shape. We perform full quantum-mechanical scattering calculations and find excellent agreement with experimental results. We also carry out semiclassical calculations where the conductance is given as a sum over all classical trajectories between the leads, each of the trajectories carrying a quantum-mechanical phase. We unambiguously demonstrate that the characteristic frequencies of the oscillations in the transmission and reflection *amplitudes t* and *r* are related to the *length distribution* of the classical trajectories between the leads, whereas the frequencies of the *probabilities* $T=|t|^2$ and $R=|r|^2$ can be understood in terms of the *length difference distribution* in the pairs of classical trajectories. We also discuss the effect of nonclassical ''ghost'' trajectories, i.e., trajectories that include classically forbidden reflection off the lead mouths.

DOI: 10.1103/PhysRevE.66.026217 PACS number(s): 05.45.Mt, 03.65.Sq, 73.23.Ad

I. INTRODUCTION

The low-temperature conductance of nanoscaled semiconductor quantum dots (often called quantum billiards) is dominated by quantum-mechanical interference of electron waves giving rise to reproducible conductance oscillations [1–10]. Theoretical and experimental studies of the conductance oscillations have been concentrated on both statistical and geometry-specific features [1–17]. Analyses of the statistical aspects of the conductance are commonly based on the random matrix theory or similar stochastic methods [12]. In order to provide an interpretation of the geometry-specific features in oscillations in a billiard of a given shape; different, and sometimes conflicting, approaches have been used [1–11,14–17]. Very often the interpretation of the conductance is not directly based on transport calculations. Consequently, the explanation of the characteristic peaks in the conductance spectrum has had rather speculative character. In contrast, the semiclassical approach [13–19] represents one of the most powerful tools to study the geometry-specific scattering as it allows one to perform transport calculations for structures of arbitrary geometry. At the same time, the semiclassical approach can provide an intuitive interpretation of the conductance in terms of classical trajectories connecting the leads, each of them carrying the quantum-mechanical phase.

In this paper, we present experimental studies of geometry-specific quantum scattering in microwave billiards of a given shape using both an exact quantum mechanical as well as a semiclassical analysis. The physics and modeling of microwave cavities are conceptually similar to that of semiconductor quantum dots because of the similarity between the Schrödinger and Helmholtz equations [19,20]. At the same time, the microwave cavities provide a unique opportunity to control the precise shape of the billiard. This is not possible for the semiconductor quantum dots where the actual shape of the potential always remains unknown [21]. Second, for the microwave billiards one can routinely access the phase information (i.e., measuring the complex transmission and reflection *amplitudes t* and *r*) whereas for the case of quantum dots one typically measures the transmission *probabilities* $T=|t|^2$ only. Third, the effect of inelastic scattering is of much lesser importance for the microwave cavities than for quantum dots where the phase breaking processes can reduce the phase coherence length significantly. Note that a billiard system of the same shape as that studied here (realized as a semiconductor quantum dot) was investigated in Refs. [5,16]. It has been demonstrated [16] that strong inelastic scattering has lead to the suppression of major characteristic peaks in the transmission spectrum as well as to the strong reduction of the amplitude of the oscillations.

Our semiclassical (SC) analysis of the experimental spectrum of the microwave billiard unambiguously demonstrates that the characteristic frequencies of the oscillations in the transmission and reflection *amplitudes t* and *r* are related to the *length distribution* of the classical trajectories between the leads, whereas the frequencies of the *probabilities* $T=|t|^2$ and $R=|r|^2$ can be understood in terms of the *length difference distribution* in all pairs of classical trajectories. To the best of our knowledge, this provides the first *unambiguous* identification of the specific frequencies experimentally observed in a billiard of a given shape.

II. BASIC THEORY

The dynamics of an electron in a two-dimensional quantum dot is governed by the Schrödinger equation

$$\left(\frac{\hbar^2}{2m}\nabla^2+E\right)\psi(x,y)=0, \tag{1}$$

where the wave function vanishes on the boundary $\psi=\mathbf{0}$, E is the electron Fermi energy and the potential inside the billiard is assumed to be zero. This equation has the same form as the Helmholtz equation governing the dynamics of the lowest TM mode in microwave billiards [19].

In the absence of a magnetic field, the transmission amplitude t_{nm} is given by the projection of the retarded Green function $G=(H-E)^{-1}$ onto the transverse wave functions $\phi_n(y)$ in the incoming and outgoing leads [22],

$$t_{mn}(k) = -i\hbar\sqrt{v_n v_m} \times \int dy_1 \int dy_2 \phi_n^*(y_1)\phi_m(y_2)G(y_1,y_2,k), \tag{2}$$

where v_n is the longitudinal velocity for the mode n and k is the wave vector. The total transmission coefficient $T=\Sigma_{mn}T_{mn}$ is a sum over all transmission probabilities of modes m propagating in one lead to modes n propagating in the other; T_{mn} is the square modulus of the transmission amplitude, $T_{mn}=|t_{mn}|^2$.

The quantum-mechanical computations have been performed using a recursive Green's function technique based on the Dyson equation [23]. In semiclassical computations, the quantum-mechanical Green function is replaced by its semiclassical approximation [18,19]. The semiclassical transmission amplitude can be represented by the form [14–17]

$$t_{mn}^{SC}(k) = \sum_s A_{mn}^s e^{ikl_s}, \tag{3}$$

where s denotes a classical trajectory of length l_s between the two leads; A_{mn}^s is an amplitude factor that depends on the density of trajectories, mode number, entrance and exit angles, etc. The details of the semiclassical calculations are given in Ref. [17].

The conductance oscillations are most conveniently analyzed in terms of the length spectrum given by the Fourier transform (FT)

$$\tilde{f}(\ell) = \int dk f(k) e^{-ik\ell}. \tag{4}$$

Due to the rapidly varying phase factor in the exponent of Eq. (3), the length spectrum of the SC transmission amplitude $\tilde{t}_{mn}^{SC}(\ell)$ is obviously peaked at the lengths $\ell=l_s$ of the trajectories between the leads. This behavior of the length spectrum is well understood and has been numerically verified for a number of different model billiards with leads [14–16].

Using Eq. (3), the transmission probability can be written in the form

$$T_{mn}^{SC}=|t_{mn}^{SC}|^2=\sum_s |A_{mn}^s|^2+\sum_{s,s'} A_{mn}^s \; A_{mn}^{s'} * e^{ik(l_s-l_{s'})}. \tag{5}$$

The first (slowly varying) term represents, in the limit of a large mode numbers in the leads, the classical transmission probability. The second (oscillating) term describes quantum corrections to the classical transmission due to interference between paths s and s'. The length spectrum of the transmission probability $\tilde{T}_{mn}^{SC}(\ell)$ is obviously peaked at the length difference $\ell=l_s-l_{s'}$ in all pairs of trajectories between the leads. Thus, identification of the characteristic frequencies in the probabilities reduces to the analysis of the path difference distribution in a billiard with a given lead geometry [14,17].

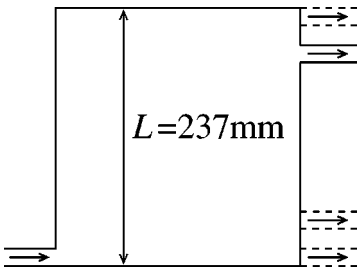

FIG. 1. Sketch of the resonator used in the experiment (in scale). Measurements have been taken for four different positions of the outgoing wave guide as indicated in the figure.

III. EXPERIMENT

Figure 1 shows a sketch of the microwave resonator used in the experiments. The microwaves enter the resonator through a waveguide at a fixed position on one side, and leave the resonator on the opposite side through another waveguide, which could be attached at four different positions indicated in the figure. Commercially available waveguides were used, with coupling antennas at the end and closed by a microwave absorber. The experimental approach uses the fact that in quasi-two-dimensional resonators there is a one-to-one correspondence with quantum mechanics as long as the frequency is smaller than $\nu_{\max}=c/2d$, where d is the resonator height [19]. In particular, the quantum-mechanical transmission amplitude t introduced above, corresponds directly to the transmission amplitude for an electromagnetic wave to pass from the entrance to the exit waveguide. In the present experiment the height was $d=7.8$ mm, i.e., the billiard was quasi-two-dimensional for $\nu<19$ GHz. More experimental details can be found in Ref. [24]. Transmission spectra, including modulus and phase, were taken in the frequency range 10 GHz$<\nu<$18 GHz for the four available positions of the outgoing waveguide. In the whole frequency range there is only one propagating mode in the waveguide. As an example, Fig. 2 shows the real and imaginary parts of a typical transmission amplitude $t(\nu)$ obtained in this way, as well as the transmission probability $T(\nu)=|t(\nu)|^2$.

IV. RESULTS AND DISCUSSION

Figure 3 shows the experimental and calculated data for the Fourier transformed transmission and reflection *amplitudes*, $\tilde{t}_{11}(\ell)$ and $\tilde{r}_{11}(\ell)$. The agreement between the experimental results and the exact quantum-mechanical (QM) calculations is very good. The SC transport calculations allow us to identify the characteristic peaks in the length spectrum in terms of classical trajectories connecting the billiard leads. Indeed, each peak in the SC spectrum represents a contribution from a particular classical trajectory, as illustrated in the insets. However, because of the approximate nature of the

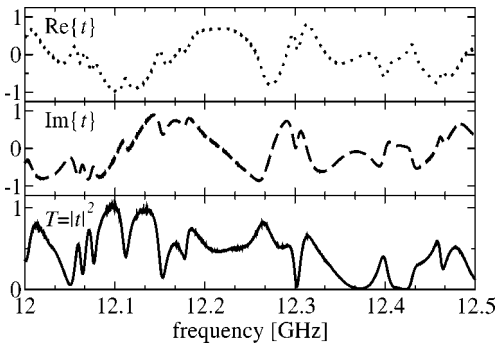

FIG. 2. Real and imaginary parts of a typical transmission amplitude $t(\nu)$ (dotted and dashed lines, respectively). The solid line shows the transmission probability $T(\nu)=|t|^2$. The total interval of frequency variation is 10 GHz$<\nu<$18 GHz. The frequency resolution is 200 kHz.

semiclassical approximation, the heights of the SC and QM peaks do not agree fully with each other.

Furthermore, the experimental data as well as the QM calculations show the presence of peaks that are absent in the SC calculations (for example, the peaks at $l\approx 5.5,8.8,10.5$ in the reflection amplitude). These are so-called ''ghost'' trajectories, i.e., trajectories that include a classically forbidden reflection off the lead mouths [14]. For example, the peak in the reflection amplitude at $l\approx 8.8$ is caused by the trajectory with the length $l=4.4$ which, after one revolution in the billiard, is reflected back at the exit by the lead mouth, so that it makes one more revolution; and its total length is then $L\approx 4.4\times 2=8.8$. Such nonclassical trajectories are not included in the standard semiclassical approximation.

The ghost trajectories are more important for reflection than for transmission. This is due to the fact that each ghost trajectory, manifesting itself in the reflection, bounces off the lead mouth only once, whereas each ghost trajectory, contributing to the transmission, has to bounce off the lead mouth twice. As a result, the amplitude of such a trajectory with two nonclassical bounces is obviously lower than that with only one bounce.

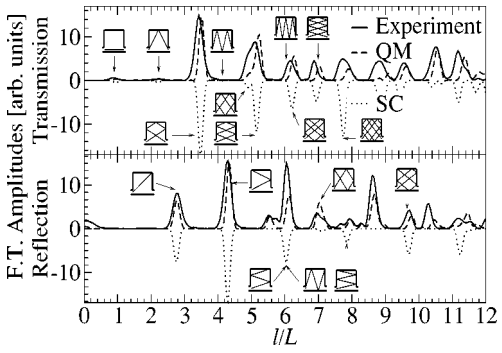

FIG. 3. Fourier transform of the experimental and calculated quantum-mechanical (QM) transmission and reflection *amplitudes*, $\tilde{t}_{11}(\swarrow)$ and $\tilde{r}_{11}(\swarrow)$, for the square billiard with opposite leads. The lower curve shows corresponding semiclassical (SC) results, plotted with a negative sign for the sake of clarity. The characteristic peaks are identified in terms of classical transmitted and reflected trajectories. Peaks in the reflection amplitude at $l\approx 5.5L$, $8.8L$ are due to ''ghost'' trajectories that include a classically forbidden reflection off the lead mouths. The range of the frequency variation corresponds to one propagating mode in the leads. The insets show the schematic geometry of the experimental microwave billiard.

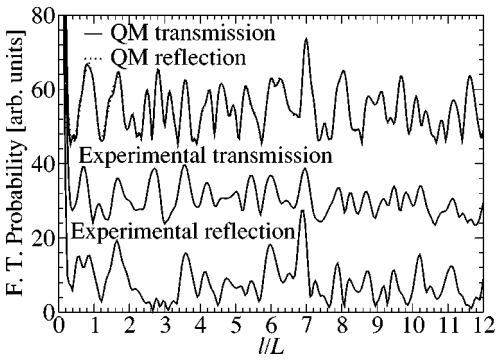

FIG. 4. Fourier transform of the experimental and calculated quantum-mechanical (QM) transmission and reflection *probabilities*, $\tilde{T}_{11}(\swarrow)$ and $\tilde{R}_{11}(\swarrow)$, for the square billiard with opposite leads.

The Fourier transforms of the experimental and calculated QM transmission and reflection *probabilities*, $\tilde{T}_{11}(\swarrow)$ and $\tilde{T}_{11}(\swarrow)$, are shown in Fig. 4. The correspondence between the theoretical and experimental probabilities is also rather good. Note that because of the current conservation requirement, $R+T=1$, the variation of the transmission is opposite to that of reflection, $\delta T=-\delta R$. As a result, the FTs of the *calculated* QM transmission and reflection probabilities are practically identical. This is, however, not the case for the *experimental* transmission and reflection probabilities, because of the presence of some absorption in the system. As we neither include absorption nor inelastic scattering in the theoretical calculations, this is the reason for some discrepancy existing between the QM calculations and the experiment.

In contrast to the case of SC and QM *amplitudes*, the agreement between the SC and QM *probabilities* is only marginal (therefore we do not show the SC results here). Because the probabilities are the squared moduli of the amplitudes, $T=|t|^2$, the discrepancy that exists between the SC and QM *amplitudes*, see Fig. 3, becomes much more pronounced for the *probabilities* (a detailed analysis of the discrepancy between the SC and QM approaches is given in Ref. [17]). Furthermore, the interval of the frequency variation (limited to one propagating mode in the leads) is not wide enough to ensure reliable statistics for the *probabilities*. The calculations demonstrate that with a wider frequency interval the characteristic peaks in the FT spectrum of the probabilities $\tilde{T}(\swarrow)$ and $\tilde{R}(\swarrow)$ become better resolved and the agreement between the QM and SC results improves significantly. Experimentally, however, it is not possible to access the frequency range beyond one propagating mode in the leads.

In order to provide an SC interpretation of the probabilities in the available frequency interval (limited to one propagating mode), we average over four different lead geometries, see Fig. 5. Such averaging is justified because the characteristic frequencies of the oscillations in a square bil-

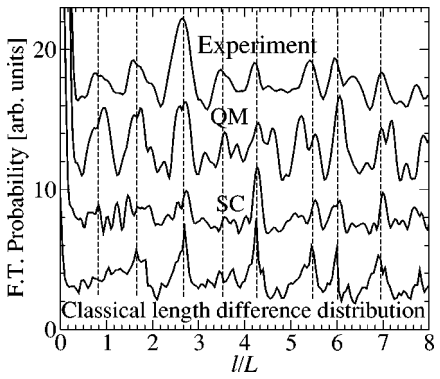

FIG. 5. Fourier transform of the experimental, quantum-mechanical (QM) and semiclassical (SC) transmission *probabilities* $\langle \tilde{T}_{11}(\not\subset) \rangle$ in a square billiard averaged over four different lead positions. The characteristic frequencies in the transmission *probabilities* can be understood in terms of the *length difference distribution* in the pairs of classical trajectories between the leads (the lower curve). Vertical dashed lines serve as guides for the eye.

liard have been shown to be rather insensitive to the lead positions [16]. This in turn is related to the fact that the classical length difference distribution is also not sensitive to the lead positions. The averaged Fourier transform of the QM probabilities, $\langle \tilde{T}_{11}(\not\subset) \rangle$, shows pronounced peaks in the FT, which are in a good agreement with the corresponding experimental ones. The correspondence between the averaged QM and SC results is also rather good. According to the SC approach, the characteristic peaks in the SC spectra can be understood in terms of the length differences in pairs of classical trajectories connecting the leads, see Eq. (5). This is demonstrated in Fig. 5 where the experimental and calculated spectra are compared to the classical length difference distribution between the leads. This provides us with a semiclassical interpretation of the calculated QM (and therefore observed) conductance fluctuations. We would like to stress that this explanation of the characteristic frequencies in the conductance is based on transport calculations for the *open* dot and is thus not equivalent to the rather common point of view when the observed frequencies in the conductance oscillations of an open dot are assigned to the contributions from specific periodic orbits in a corresponding closed dot [1–9,11].

V. CONCLUSIONS

We present experimental studies of the geometry-specific quantum scattering in a microwave billiard of a given shape. We perform full quantum-mechanical (QM) scattering calculations and find an excellent agreement with the experimental results. We also carry out semiclassical (SC) calculations where the conductance is given as a sum of all classical trajectories between the leads, each of them carrying the quantum-mechanical phase. Our results thus provide an *unambiguous* identification of the specific frequencies of the oscillations observed in a billiard of a given shape.

ACKNOWLEDGMENTS

Financial support from the National Graduate School in Scientific Computing (T.B.) and the Swedish Research Council (I.V.Z.) is acknowledged. The experiments were supported by the Deutsche Forschungsgemeinschaft.

[1] C. Marcus *et al.*, Phys. Rev. Lett. **69**, 506 (1992).
[2] A.M. Chang *et al.*, Phys. Rev. Lett. **73**, 2111 (1994).
[3] M. Persson *et al.*, Phys. Rev. B **52**, 8921 (1995).
[4] J.P. Bird *et al.*, Europhys. Lett. **35**, 529 (1996).
[5] I.V. Zozoulenko *et al.*, Phys. Rev. B **55**, 10 209 (1997); I.V. Zozoulenko and K.-F. Berggren, *ibid.* **56**, 6931 (1997).
[6] R. Akis, D.K. Ferry, J.P. Bird, Phys. Rev. Lett. **79**, 123 (1997); I.V. Zozoulenko and T. Lundberg, *ibid.* **81**, 1744 (1998).
[7] L. Christensson *et al.*, Phys. Rev. B **57**, 12 306 (1998).
[8] P. Bøggild *et al.*, Phys. Rev. B **57**, 15 408 (1998).
[9] I.V. Zozoulenko *et al.*, Phys. Rev. B **58**, 10 597 (1998).
[10] I.V. Zozoulenko *et al.*, Phys. Rev. Lett. **83**, 1838 (1999).
[11] Y. Takagaki and K.H. Ploog, Phys. Rev. E **62**, 4804 (2000).
[12] For a review, see, e.g., C.W.J. Beenakker, Rev. Mod. Phys. **69**, 731 (1997).
[13] W.H. Miller, Adv. Chem. Phys. **25**, 69 (1974); R. Blümel and U. Smilansky, Phys. Rev. Lett. **60**, 477 (1988); R.A. Jalabert, Harold U. Baranger, and A.D. Stone, *ibid.* **65**, 2442 (1990).
[14] C.D. Schwieters, J.A. Alford, and J.B. Delos, Phys. Rev. B **54**, 10 652 (1996).
[15] L. Wirtz, J.-Z. Tang, and J. Burgdörfer, Phys. Rev. B **56**, 7589 (1997).
[16] T. Blomquist and I.V. Zozoulenko, Phys. Rev. B **61**, 1724 (2000).
[17] T. Blomquist and I.V. Zozoulenko, Phys. Rev. B **64**, 195301 (2001); T. Blomquist, Phys. Rev. B (to be published); e-print cond-mat/0205287.
[18] M. C. Gutzwiller, *Chaos in Classical and Quantum Mechanics* (Springer-Verlag, New York, 1991).
[19] H.-J. Stöckmann, *Quantum Chaos: An Introduction* (Cambridge University Press, Cambridge, England, 1999).
[20] Y.-H. Kim *et al.*, Phys. Rev. B **65**, 165317 (2002).
[21] A. Fuhrer *et al.*, Phys. Rev. B **63**, 125309 (2001).
[22] See, e.g., S. Datta, *Electronic Transport in Mesoscopic Systems* (Cambridge University Press, Cambridge, England, 1995).
[23] I.V. Zozoulenko, F.A. Maaø, and E.H. Hauge, Phys. Rev. B **53**, 7975 (1996); **53**, 7987 (1996); **56**, 4710 (1997).
[24] U. Kuhl *et al.*, Eur. Phys. J. B **17**, 253 (2000).